Towards Reduced-Order Models for Online Motion Planning and Control of UAVs in the Presence of Wind

Ashray A. Doshi, Surya P. Singh and Adam J. Postula
The University of Queensland, Australia
{a.doshi, spns}@uq.edu.au, adam@itee.uq.edu.au

Abstract

This paper describes a model reduction strategy for obtaining a computationally efficient prediction of a fixed-wing UAV performing waypoint navigation under steady wind conditions. The strategy relies on the off-line generation of time parametrized trajectory libraries for a set of flight conditions and reduced order basis functions functions for determining intermediate locations. It is assumed that the UAV has independent bounded control over the airspeed and altitude, and consider a 2D slice of the operating environment. We found that the reduced-order model finds intermediate positions within 10% and at speeds of 10x faster than clock-time (even in wind conditions in excess of 50% of the UAV's forward airspeed) when compared against simulation results using a medium-fidelity flight dynamics model. The potential of this strategy for online planning operations is highlighted.

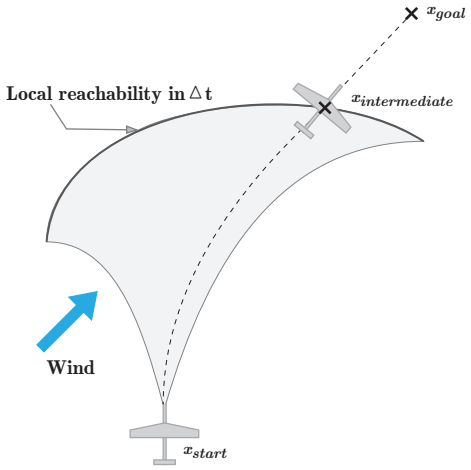

Figure 1: UAV forward simulation for the estimation of final position in a fixed time given an initial and a desired waypoint under windy conditions.

1 Introduction

The use of small fixed-wing Unmanned Aerial Vehicles (UAV) is becoming increasingly widespread in challenging urban applications such as law enforcement, powerline monitoring, disaster management and surveillance. In the case of fixed-wing aircraft, a forward speed greater than its stall speed (Vs) is required to maintain flow over its wings and generate lift. Turns are executed by banking and diverting the horizontal component of lift in the direction of the turn. This limits the rates of translation of the aircraft. Online motion planning of UAVs is an active area of research due to the future role of UAVs in challenging urban environments which are subject to large magnitude, constant dynamic wind disturbances.

The main objective of this paper is to demonstrate the feasibility of a linearized computational strategy based on polynomial basis functions and a database of reduced-order information, for the prediction of flight position and response in various wind conditions including those that exceed the disturbance rejection of the autopilot and would require rerouting. The proposed computational strategy is particularly suitable for assisting motion planning as these algorithms require numerous forward model predictions.

Inclusion of features such as sense and avoid [Carnie *et al.*, 2006] means that the computational complexity associated with re-planning is detrimental to the outcome of the planning strategy. If previously unknown obstacles are detected, a replan has to be carried out in real-time. Sampling based methods such as Rapidly-exploring random trees (RRTs) introduced in [Kuffner Jr and LaValle, 2000] are increasingly becoming popular in UAV applications. RRTs were used to perform motion planning in the output-space (waypoints) by [Cummings *et al.*, 2010] for multiple UAVs in a cluttered environment. Sampling-based methods in output-space use a forward model to estimate the future states given a desired position input

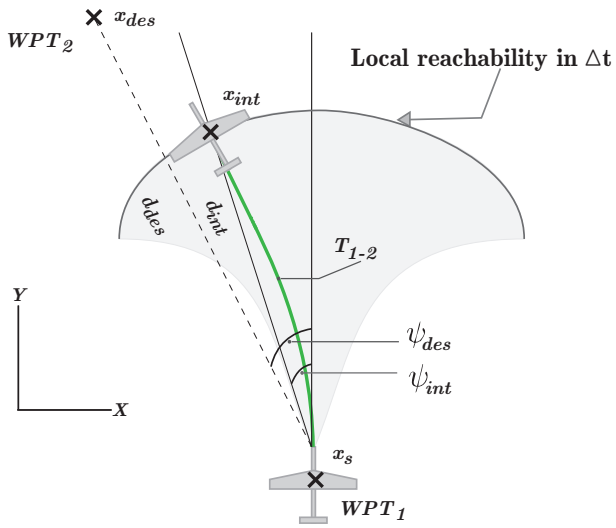

Figure 2: Trajectory estimation and local reachability between waypoints. The intermediate position ψ_{int} at a given time horizon (Δt) may be approximated as a local heading angle ψ_{int} towards a desired target waypoint.

state.

This introduces a Reduced-order Forward Model (RFM) that predicts the position of a UAV on a local time horizon, given a waypoint command and a local wind estimate. This is illustrated in Figure 1 where the UAV currently at x_{start} is following a waypoint x_{goal} in the presence of wind. An approximate model can be used to predict the position $x_{intermediate}$ in time Δt. The method can be useful for applications that require a computationally efficient and accurate prediction, taking into account the UAV dynamics in detail.

In related work, Dubins curves are arguably the most commonly used model approximations for UAV path planning [Sujit *et al.*, 2008] [Hwangbo *et al.*, 2007]. Also, the use of trajectory primitives was described in [Frazzoli *et al.*, 2005]. However, these do not take into account wind disturbance and asymmetries that may exist in the UAV's dynamics. Fixed-wing UAV dynamics can be accurately approximated using full state models [Stevens and Lewis, 2003] and [Nelson, 1989]. JSBSim [Berndt, 2004] is a C++ implementation of a full flight dynamics model that allows batch simulations. However, full flight dynamics models can be computationally expensive and infeasible for online operations.

The paper is organized as follows. In Section 2, we outline the Reduced-Order Forward Model (RFM) approach. In Section 3 simulation results are presented and the RFM performance is analyzed. In Section 4 we outline some applications of this approach. Conclusions and future work are presented in Section 4.

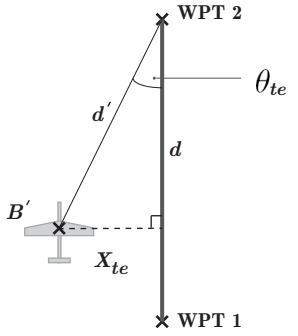

Figure 3: Cross-track error minimization used by the UAV autopilot for navigation.

2 Reduced-Order Forward Model

In order to address computational efficiency during online motion planning for small UAVs, an approximate forward model is proposed that takes into account both closed-loop feedback controller (autopilot) effort, as well as steady wind disturbance. A Reduced-Order Forward Model (RFM) was approximated such that given a set of initial conditions and an input state u, the output is the prediction of the UAV position in time Δt.

2.1 Waypoint Autopilot design

The limitations of inner-loop feedback controllers in tracking a given trajectory can be detrimental to the outcome of a motion plan while planning in output-space. For this paper, we focus on our approach in accounting for these limitations in the RFM, rather than improving the performance of the feedback controllers.

A cascaded PID-based autopilot similar to [Eng, 2011] was implemented for the purpose of the experiments. One of the functions of an autopilot is the ability to track a path described by a straight line joining two waypoints. Consider the UAV currently at B' (Figure 3) *en route* to WPT2 from WPT1, with the course to follow given by the solid line joining the two waypoints. The navigation cross-track error (X_{te}) is given by

$$X_{te} = d' \times \sin(\theta_{te}) \tag{1}$$

Where d' is the distance between the current position and goal waypoint. The navigation algorithm minimizes X_{te} using a PD-controller to give the desired heading (ψ_d) set-point, which is tracked by banking the aircraft. The rudder is commanded via a PI-controller in order to minimize sideslip (β) and perform co-ordinated turns. Airspeed and altitude hold modes were implemented using PID-controllers.

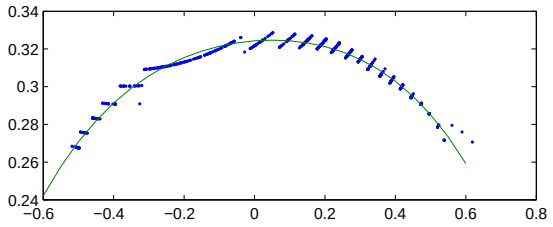

Figure 4: UAV local reachability curve in time Δt can be described by the polynomial p_1.

2.2 Training and RFM Estimation

Training data was obtained by carrying out batch simulations using an open-source 6-DOF flight dynamics model called JSBSim [Berndt, 2004]. An autopilot was implemented in C that took aircraft states from JSBSim and returned actuator deflections in order to follow a given trajectory. The small fixed-wing UAV used for simulation was the Sig Rascal model that is included in the software. The autopilot in section 2.1 was commanded to follow waypoints that were randomly sampled in $\mathbb{R}^2$ such that

$$d_a = (V_a + |W|) \times \Delta t \tag{2}$$

$$\sqrt{(x_k - x_0)^2 + (y_k - y_0)^2} \; > d_a \tag{3}$$

where W is the maximum magnitude of wind in any direction during a given flight leg. The autopilot was configured such that the bank angle was limited to ϕ_{max} $= \pm 0.69$ radian. The airspeed (V_a) and the altitude were held constant at 45 knots and 400 feet respectively.

The initial and final aircraft states after $\Delta t = 10$ seconds (RFM horizon) were recorded as training data. Simulations were carried out for wind magnitudes of [0, 5, 10, 15, 20, 25, 30] knots, and blowing from [0, 90, 180, 270] degrees. For each wind condition, 1000 batch simulations were carried out with randomly sampled desired waypoints.

Prediction under nominal Conditions

The training data consists of the initial UAV position $(x_s, y_s, \psi_s)_k$, the desired waypoints $(x_{des}, y_{des}, \psi_{des})_k$, and the final position $x_{int} = (x_{int}, y_{int}, \psi'_{int})_k$ on the reachability horizon at Δt. For each data set

$$\psi_{des} = \tan^{-1} \frac{x_{des} - x_s}{y_{des} - y_s} \tag{4}$$

$$\psi_{int} = \tan^{-1} \frac{x_{int} - x_s}{y_{int} - y_s} \tag{5}$$

$$d_{des} = \sqrt{(x_{des} - x_s)^2 + (y_{des} - y_s)^2} \tag{6}$$

$$d_{int} = \sqrt{(x_{int} - x_s)^2 + (y_{int} - y_s)^2} \tag{7}$$

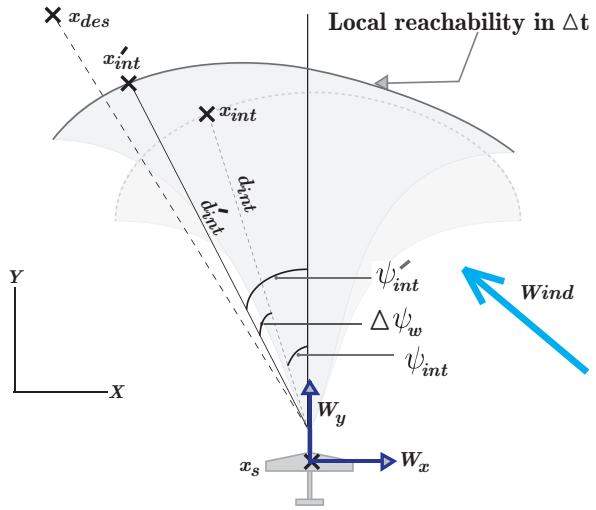

Figure 5: UAV initially at x_s given a desired waypoint x_{des} tracks to a final position of x_{int} in zero wind conditions. When the UAV is subject to wind, the cross and tail-wind components drive the final estimate to point x'_{int}.

Where ψ_{des} and ψ_{int} are the angles subtended by the aircraft forward velocity vector to the desired waypoint, and x_{int} respectively. The first step in approximating x_{int} was to fit the local reachability curve using the training data under zero wind conditions. The local reachability curve was estimated as a 3^{rd} order polynomial p_1 using the data sets of ψ_{int} and d_{int} at $|W| = 0$ (Figure 4) Let

$$\Delta\psi = \psi_{des} - \psi_{int}. \tag{8}$$

From equation 1, it is noted that the input parameters for our navigation algorithm include d_{des} and ψ_{des}. Consider the following equation

$$a_1 + a_2 \times \psi_{des} + a_3 \times d_{des} = \Delta\psi \tag{9}$$

a_i can be determined using linear least squares regression on the training data, we determine an estimation function for $\Delta\psi$ which can be seen as a ground-track heading error in navigating to the desired waypoint within Δt. The use of $\Delta\psi$ in the forward model approximation can be found in Section 2.3.

Wind Correction

In this section, we estimate a skew function that relates the offsets caused due to the effect of steady wind (no gust), to the position estimates found the zero wind conditions. We consider a flat wind model and assume that the vertical component of wind is zero. Given the same time horizon Δt, a tail-wind would increase the UAV's ground speed causing it cover more distance as compared

with no wind conditions. This is illustrated in (Figure 5). Similarly, a cross-wind would cause an offset to the ground-track heading $\Delta\psi$, and associated navigation errors. In order to simplify the skew function, we do not consider instantaneous wind effects through out the trajectory. Instead, only the cross and tail wind components at the initial position and orientation (x_s) are considered while identifying the skew function.

Consider the following equations

$$b_1 + b_2 \times W_x + b_3 \times W_y = \Delta\psi_w \quad (10)$$

$$c_1 + c_2 \times W_x + c_3 \times W_y = \Delta d_w \quad (11)$$

Where W_x and W_y are the magnitudes of wind in the x and y directions. $\Delta\psi_w$ and Δd_w are the offsets due to wind on d_{int} and $\Delta\psi$ respectively. b_i and c_i can be determined by using linear least squares regression on the training data.

2.3 Reduced-Order Forward Model Usage

In Section 2.2 we used training data to estimate parameters required for our Reduced-Order Forward Model (RFM). In this section, we describe the usage of the RFM for predicting an approximate future position and heading in a time horizon Δt. We assume that the wind magnitude and direction can be estimated using direct methods and on-board sensors using methods similar to [van den Kroonenberg *et al.*, 2008]. At run-time, given an initial state x_s, desired state x_{des}, and a wind magnitude and direction, following are the steps that need to be taken in order to predict the future state (x_{int}) using the reduced-order forward model in Section 2.2:

Step 1:
Given an initial position (x_s, y_s, ψ_s), and a desired waypoint $(x_{des}, y_{des}, \psi_{des})$, ψ_{des} and d_{des} can be determined using Equations 4 and 7 respectively.

Step 2:
Values of a_i were determined by using the training data in Section 2.2. Substituting the values of a_i, ψ_{des} and d_{des} (from Step 1) into equation 9, we obtain an approximation of $\hat{\Delta\psi}$ before applying wind correction.

Step 3:
Re-arranging equation 8, $\hat{\psi_{int}} = \psi_{des} - \hat{\Delta\psi}$. Using equation 9 and the value of $\hat{\Delta\psi}$ found in the previous step, we obtain the approximate value of $\hat{\psi_{int}}$. It can be noted that under no wind conditions, $\hat{\psi_{int}}$ is an approximation of the angle between the UAV initial forward velocity vector and UAV final position at time Δt.

Step 4:
Evaluating polynomial p_1 approximated in Section 2.2 at $\hat{\psi_{int}}$ gives the value of $\hat{d_{int}}$, which is the displacement of the UAV from its initial position towards the desired waypoint at time Δt.

In steps 3 and 4, we have found the approximate position and heading of the UAV on the local reachability curve (Figure 2) in time Δt in no wind conditions. In presence of wind (Figure 5), offsets due to wind can be approximated as follows:

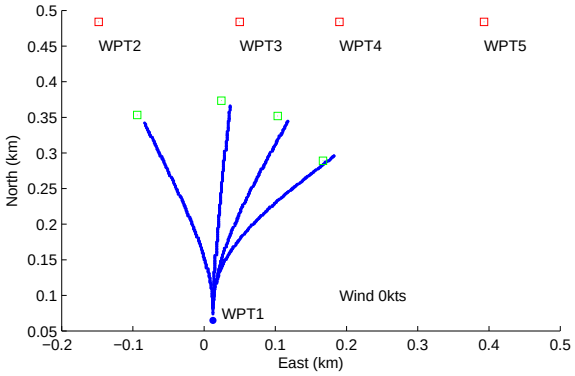

Figure 6: Comparison of the RFM approximation with JSBSim simulation (No Wind). Simulation starts at WPT1 and the autopilot is commanded to fly to waypoints (WPT) 2, 3, 4 and 5. Green points are predicted by the RFM in Δt = 10s, and the blue curves are the trajectories flown by JSBSim in 10s

Step 5:
Values of b_i and c_i were determined by using the training data in Section 2.2. Evaluating Equations 10 and 11, we get the approximate values for $\Delta\hat{\psi}_w$ and $\Delta\hat{d}_w$ which are offsets on the positions found in steps 3 and 4.

Step 6:
Applying the offsets found in step 5, the final approximations of $\Delta\hat{\psi}'_w$ and $\Delta\hat{d}'_w$ (illustrated in Figure 5) can be found by using the following

$$\Delta\hat{\psi}'_w = \hat{\psi_{int}} + \Delta\hat{\psi}_w \quad (12)$$

$$\Delta\hat{d}'_w = \hat{d_{int}} + \Delta\hat{d}_w \quad (13)$$

3 RFM Validation and Simulation

We demonstrate our method in simulation by comparing the performance of the RFM against simulations in a full flight dynamics model (JSBSim). The RFM in Section 2.3 was validated by carrying out batch simulations of a small fixed-wing UAV model (Sig Rascal) under various wind conditions. Similar to Section 2.2, 1000 random waypoints were followed using the same autopilot in Section 2.1 at wind magnitudes of 0, 13 and 23 knots (different to the training set) each blowing from North, East, South and West. The test data also includes desired waypoints that require a constant bank angle saturation during the entire flight leg.

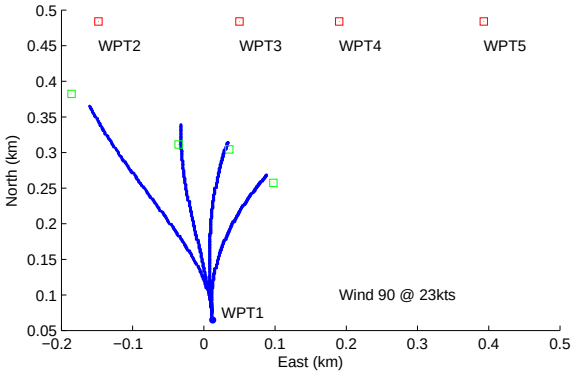

Figure 7: Wind blowing from the East at 23 knots (Green squares are predictions and the blue lines are flight traces)

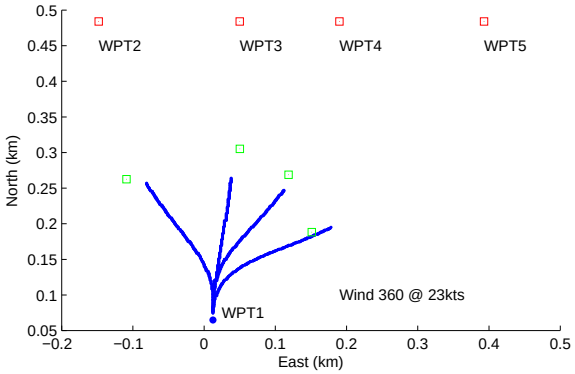

Figure 9: Wind blowing from the North at 23 knots (Green squares are predictions and the blue lines are flight traces)

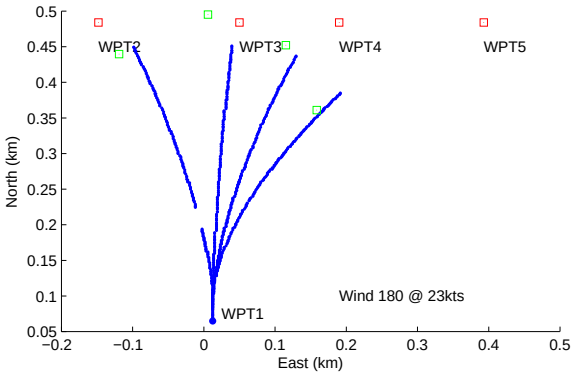

Figure 8: Wind blowing from the South at 23 knots (Green squares are predictions and the blue lines are flight traces)

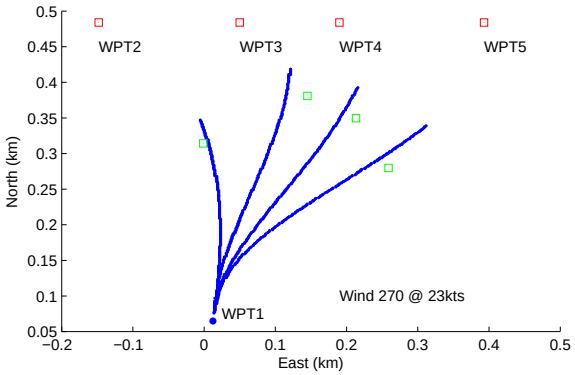

Figure 10: Wind blowing from the West at 23 knots (Green squares are predictions and the blue lines are flight traces)

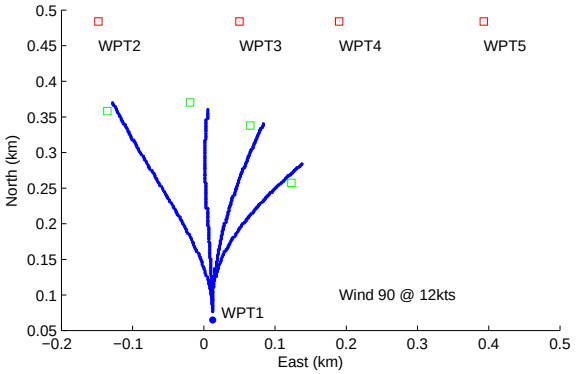

Figure 11: Wind blowing from the East at 12 knots (Green squares are predictions and the blue lines are flight traces)

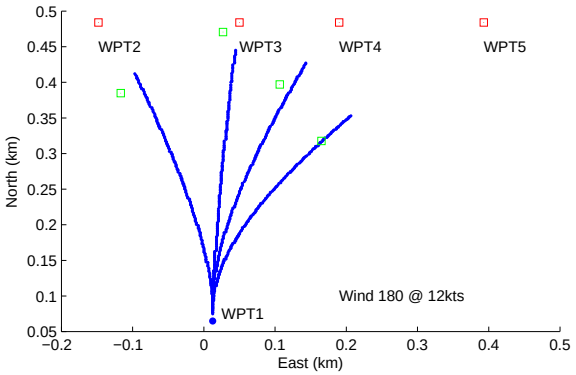

Figure 12: Wind blowing from the South at 12 knots (Green squares are predictions and the blue lines are flight traces)

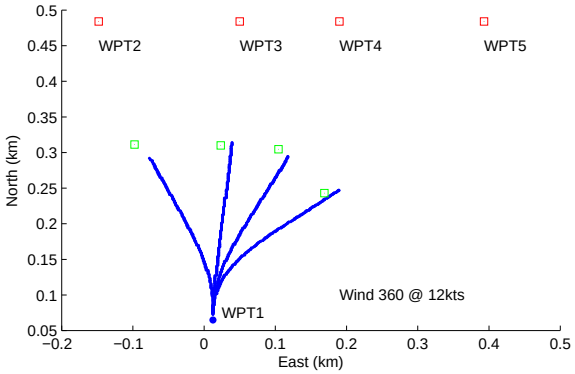

Figure 13: Wind blowing from the North at 12 knots (Green squares are predictions and the blue lines are flight traces)

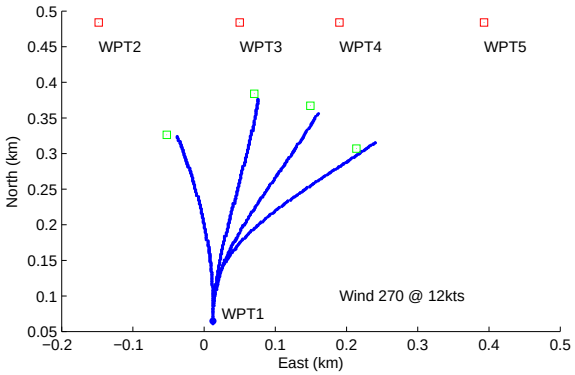

Figure 14: Wind blowing from the West at 12 knots (Green squares are predictions and the blue lines are flight traces)

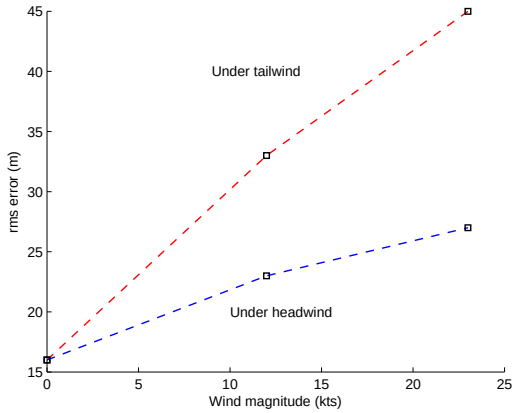

Figure 15: RMS error in estimation using the RFM. The red dashed line indicates the RMS error of the prediction of UAV flight under tail-wind which can reach 45m at 24kts. This is significantly more than the RMS error of estimation of cases where the UAV is navigating under a head-wind (blue).

RFM Prediction Performance

In Figure 6, four test cases of RFM predictions are plotted for simplicity of illustration. It can be seen that under zero wind conditions, the RFM prediction closely matches that of the full flight dynamics model with an RMS error of 16m. It can be observed that the prediction error increases with increase in wind magnitude. In the case of prediction of UAV position under-headwind, the RMS error increases from 22m at a wind magnitude of 13kts (figure 15), up to 25m at 24kts (half the UAV's airspeed). However, under tail-wind, the RMS error increases from 33m at 13kts, up to 44m at 24kts. The fact that prediction errors are smaller for cases where the UAV navigates under the influence of a head-wind, when compared to tail-wind will be investigated in future work.

Run-time Performance

The computation time on an Intel i7 2.8GHz PC for the RFM is significantly less at 0.1 second per 1000 iterations, when compared to that of JSBSim which took 20 seconds.

No. of iterations	JSBSim (time)	RFM (time)
1000	20 sec	0.1 sec
3600	72 sec	0.35 sec

4 Conclusion and Future Work

We presented an approximation strategy for wind gust. We note that in stochastic motion that there is a need for multiple queries towards a goal, future work is looking at incorporating these ideas into a RRT motion planner.

References

[Berndt, 2004] J.S. Berndt. Jsbsim: An open source flight dynamics model. In *in C++. AIAA*, 2004.

[Carnie *et al.*, 2006] R. Carnie, R. Walker, and P. Corke. Image processing algorithms for uav sense and avoid. In *Robotics and Automation, 2006. ICRA 2006. Proceedings 2006 IEEE International Conference on*, pages 2848–2853. IEEE, 2006.

[Cummings *et al.*, 2010] M.L. Cummings, A.D.J.C.C. Caves, et al. *Human-automation collaborative RRT for UAV mission path planning*. PhD thesis, Massachusetts Institute of Technology, 2010.

[Eng, 2011] P. Eng. *Path planning, guidance and control for a UAV forced landing*. PhD thesis, Queensland University of Technology, 2011.

[Frazzoli *et al.*, 2005] E. Frazzoli, M.A. Dahleh, and E. Feron. Maneuver-based motion planning for nonlinear systems with symmetries. *Robotics, IEEE Transactions on*, 21(6):1077–1091, 2005.

[Hwangbo *et al.*, 2007] M. Hwangbo, J. Kuffner, and T. Kanade. Efficient two-phase 3d motion planning for small fixed-wing uavs. In *Robotics and Automation, 2007 IEEE International Conference on*, pages 1035–1041. IEEE, 2007.

[Kuffner Jr and LaValle, 2000] J.J. Kuffner Jr and S.M. LaValle. Rrt-connect: An efficient approach to single-query path planning. In *Robotics and Automation, 2000. Proceedings. ICRA'00. IEEE International Conference on*, volume 2, pages 995–1001. IEEE, 2000.

[Nelson, 1989] R.C. Nelson. *Flight stability and automatic control*. McGraw-Hill New York;, 1989.

[Stevens and Lewis, 2003] B.L. Stevens and F.L. Lewis. *Aircraft control and simulation*. Wiley-Interscience, 2003.

[Sujit *et al.*, 2008] PB Sujit, JM George, and RW Beard. Multiple uav coalition formation. In *American Control Conference, 2008*, pages 2010–2015. IEEE, 2008.

[van den Kroonenberg *et al.*, 2008] A. van den Kroonenberg, T. Martin, M. Buschmann, J. Bange, and Vörsmann. Measuring the wind vector using the autonomous mini aerial vehicle m2av. *Journal of Atmospheric and Oceanic Technology*, 25(11):1969–1982, 2008.